Hindawi
Advances in Civil Engineering
Volume 2022, Article ID 4219524, 15 pages
https://doi.org/10.1155/2022/4219524

Research Article

Use of Artificial Neural Networks and Response Surface Methodology for Evaluating the Reliability Index of Steel Wind Towers

Indira Inzunza-Aragón,[1] **Sonia E. Ruiz**,[1] **and Laura Cruz-Reyes**[2]

[1]*Institute of Engineering, Universidad Nacional Autónoma de Mexico, Coyoacan 04510 Mexico City, Mexico*
[2]*Instituto Tecnológico de Ciudad Madero, Ciudad Madero, Tamaulipas, Mexico*

Correspondence should be addressed to Sonia E. Ruiz; sruizg@iingen.unam.mx

Received 4 October 2021; Revised 21 January 2022; Accepted 21 February 2022; Published 28 June 2022

Academic Editor: Xiao Sun

The estimation of structural reliability is a process that requires a large number of computational hours when statistical data are not available since it is necessary to perform a large amount of analysis or numerical simulations to estimate parameters related to the reliability. A methodology is proposed for estimating the structural reliability index, as well as the demand and structural capacity factors inherent to the structure, given the fundamental vibration period and the height of the structure, by using artificial neural networks (ANN) and, alternatively, the response surface method (RSM). Both approaches are applied to steel wind turbine towers. For the cases studied, ANN allow evaluating the reliability index and both the demand and structural capacity factors with greater accuracy than when using RSM.

1. Introduction

The methodology proposed by SAC-FEMA [1] for the evaluation of the demand and capacity factors based on structural reliability is a basic procedure that engineers usually use; however, its application implies carrying out a large number of analyses or simulations to estimate the safety factors and the reliability index implicit in the structural designs. Due to this limitation, numerical simulation methods have been applied to obtain those factors; for example, FORM and SORM methods, together with simplified probabilistic models, consider a given limit state [2, 3], or considering material fatigue [4, 5]; however, these procedures require great numerical processing time.

In the literature, methods have been proposed to obtain the probability of failure of structures that optimize computational resources. An example is the response surface method (RSM) [6], which can be as simple as a second-order equation, up to exponential or high-order response surfaces [7, 8], and even modified techniques where heavy polynomial calibrations are applied [9], as well as the use of theoretical evidence and control points to create the response surface [10].

In recent decades, computational processes have been used to solve complex engineering problems [11, 12], such as optimization design [13, 14], structural response [15], and others. Artificial neural networks (ANN) for structural reliability analysis have been used since 1989 when Hornik et al. [16–18] proved that multilayer networks can approximate any function with a high degree of accuracy. Some other applications are as follows: Chen [19–21] uses genetic algorithms to calculate the reliability index of bridges, trusses, and flat frames; Bojorquez et al. [22] propose a methodology based on optimization to find live, dead, and earthquake load factors for design of buildings located on soft soil; Dai and Cao [23] use hybrid methods (ANN and wavelet neural network) to obtain the probability of failure of various structures; Santana Gomes [18] calculates the probability of failure of several structures using adaptive ANN and compares its results obtained with these networks

with those from Monte Carlo simulations; Wen et al. [24] optimize ANN to obtain the reliability of gas lines and compare their results with an unoptimized network and with Monte Carlo simulations; however, there are very few studies focused on the use of artificial intelligence for the calculation of structural safety factors; for example, Koopialipoor [25] uses the ant colony optimization algorithm to maximize the safety factor of retaining walls; Zeroual [26] calculates safety factors for dams, using a feedforward backpropagation network; Gordan et al. [27] obtain safety factors for retaining walls using ANN and "artificial bee colony"; and Zhang et al. [28] propose a Bayesian network for calculating pile resistance factors.

Response surface and ANN methods have focused mainly on obtaining the probability of failure of the structures; however, no efforts have been made to evaluate the structural reliability index, nor the demand and structural capacity factors implicit in wind turbine towers, which is a research gap that is addressed in the present study.

Based on the above, the main objective of this research is to propose a methodology to estimate the structural reliability index, together with the structural demand and structural capacity factors; the estimations are through ANN and alternative through RSM. The objective of the experimental analysis is to compare the performance of ANN and RSM based on accuracy. For this study, both approaches are applied, as part of the proposed methodology, only to steel wind turbine towers installed in open terrain, specifically in La Ventosa region of Oaxaca, in Mexico.

2. Reliability Analysis

Cornell et al. [1] propose a probabilistic methodology to obtain structural reliability, which is expressed in terms of the annual structural failure probability or the structural reliability index β. The objective is to obtain the probability of exceeding a structural parameter level (for example, the maximum expected displacement associated with a given intensity).

Structural reliability can be described in terms of the mean annual exceedance rate ν_F, as shown in (1), which represents the expected number of times that environmental actions d, exceed the structural capacity C, evaluated for an intensity y, according to the site environmental hazard curve $\nu(y)$ [29, 30].

$$E(\nu_F) = \int_0^\infty P[C < d|y] \left| \frac{\mathrm{d}\nu(y)}{\mathrm{d}y} \right| \mathrm{d}y. \tag{1}$$

Cornell et al. [1] propose closed equations to solve (1), and their method is based on characterizing the natural hazard $\nu(y)$ and the median structural demand $\widehat{D}$. In (2), $\nu(y)$ is a function of the intensity y and the shape parameters k and r. In (3), a and b are the shape parameters.

$$\nu(y) = ky^{-r}, \tag{2}$$

$$\widehat{D} = ay^b. \tag{3}$$

Considering the previous aspects, (1) can be rewritten in (2) and (3) [31, 32].

$$E(\nu_F) = k\left[\left(\frac{\widehat{C}}{a}\right)^{\frac{1}{b}}\right]^{-r} \cdot \exp\left\{\frac{r^2}{2b^2}\left[\sigma_{lnD}^2 + \sigma_{lnC}^2 + \sigma_{UD|y}^2 + \sigma_{UC}^2\right]\right\}, \tag{4}$$

where $\widehat{C}$ is the median of the structural capacity corresponding to a certain limit state; σ_{lnC}^2 and σ_{lnD}^2 correspond to the variances of the natural logarithm (random uncertainties) of capacity and structural demand, respectively; σ_{UC}^2 and σ_{UD}^2 represent the epistemic uncertainties of capacity and structural demand, respectively.

Once the expected number of failures per year is calculated, the probability of failure can be obtained using (5) (assuming that it is a nonhomogeneous stochastic Poisson process). From this, the reliability index β can be obtained (see (6)).

$$p_{f,T} = 1 - e^{\left[-E(\nu_F)\right]}, \tag{5}$$

$$\beta = \Phi^{-1}\left(p_{f,T}\right). \tag{6}$$

To achieve the appropriate level of reliability, it is established that the median factored capacity associated with a limit state $\widehat{C}$ must be greater than or equal to the factored demand associated with a desired annual failure rate $\widehat{D}^{\nu_o}$ [1].

$$\phi\widehat{C} \geq \gamma\widehat{D}^{\nu_o}, \tag{7}$$

where ϕ is the structural capacity factor, and γ is the structural demand factor. $\widehat{D}^{\nu_o}$ is calculated with (8), where ν_o is a desirable or target annual failure probability, a and b are parameters that characterize the demand, and k characterizes the hazard (i.e., seismic or wind).

$$\widehat{D}^{\nu_o} = a\left[\frac{\nu_o}{k}\right]^b. \tag{8}$$

The capacity and demand factors are, respectively, as follows:

$$\phi = \exp\left[-\frac{r}{2b}\sigma_{CT}^2\right], \tag{9}$$

$$\gamma = \exp\left[\frac{r}{2b}\sigma_{DT}^2\right], \tag{10}$$

where $\sigma_{CT}^2 = \sigma_{lnC}^2 + \sigma_{UC}^2$ represents the total uncertainties associated with the structural capacity, and $\sigma_{DT}^2 = \sigma_{lnD}^2 + \sigma_{UD}^2$ represents the total uncertainties corresponding to the structural demand.

The relation between factored capacity and factored demand is called the confidence factor λ. This factor indicates whether the structural design will achieve the desired performance for the limit state being reviewed. If λ is greater than or equal to 1, the structure's average annual failure rate is on the safety side [1].

3. Response Surface Method

A response surface refers to a polynomial that relates a mechanical model to its numerical response. Basically, it is an equation that relates the variables of a system with results obtained either from experimentation, numerical simulation, or theoretical data [6]. The particularity of the method is to obtain a function $g(X)$ simple enough, in grade and in the number of variables, and that, at the same time, allows solving the problem.

The second-order equation is the most used way to solve response surfaces; however, for problems that present some degree of nonlinearity, the second-order polynomial equation can be applied with the mixed terms of the variables that intervene in the function [7].

$$g(X) = A + \sum_{i=1}^{n} B_i X_i + \sum_{i=1}^{n} C_i X_i^2 + \sum_{i=1}^{n-1} \sum_{j=i+1}^{n} D_{ij} X_i X_j, \quad (11)$$

where n is the number of variables, that is, height, diameter, weight, forces, and A, B_i, C_i, and D_{ij} are unknown coefficients, which are obtained through regression analysis, such as using the least-squares method [33], or some other adjustment model that adapts to the problem.

To validate the results obtained from the response surface, the coefficient of determination R^2 is used (see (12)), which indicates the precision of the approximation between the real data and those predicted by the response surface [7].

$$R^2 = 1 - \frac{\sum_{i=1}^{P} (\overline{g}(X) - g(X))^2}{\sum_{i=1}^{P} (g(X) - \overline{g})^2}, \quad (12)$$

where P is the total number of points, and the mean value of function $\overline{g}$ is as follows:

$$\overline{g} = \frac{1}{P} \sum_{i=1}^{P} g(X_i). \quad (13)$$

In the present study, second-order response surfaces are obtained from structural reliability analysis, corresponding to 54 different models of wind turbine steel towers.

4. Artificial Neural Networks

Artificial neural networks (ANN) are algorithms designed to solve a specific problem. They imitate the human learning process, based on the configuration of the neurons of the nervous system, which are capable of learning through experience, generalizing, extending, or expanding a situation, and abstracting the characteristics of the object of study [34, 35]. McCulloch and Pitts [36] propose the first model of an artificial neural network; many ANN forms have emerged since this appearance. ANN can be classified in different ways, including the following: according to the number of layers, in single layer and multilayer [37]; by the architecture learning, in supervised [38], unsupervised [39], hybrid [40, 41], and reinforced [42, 43]; and by the data flow for the learning algorithm, in feedback and unidirectional [35].

A perceptron is the basic computational unit of an ANN. The perceptron introduction by Rosenblatt [44] was a radical innovation to this area. A study by Minsky and Papert [45] revealed that perceptrons could only learn linearly separable functions, limiting their research. In the 1980s, the works were reactivated by overcoming this limitation with the combination of perceptron layers (also called multilayer perceptron or MLP) [46]. To understand MLP, Taud [47] provides a brief introduction to a single-layer perceptron with one neuron. This perceptron works from input data x_k, provided externally or by another perceptron; then, these data are transformed through linear coefficients called "weights" w_k and a bias value b_m. From this point, the transfer function f transforms these weights to output data towards another neuron or final responses out_m as represented in (14) and Figure 1. The MLP is a unidirectional layered feedforward ANN where the information flows from the input layer to the output layer, passing through the hidden layers [48]. Each neuron connection has its own weight. For the same layer, perceptrons have the same activation function that generally is a sigmoid [47].

$$\text{out}_m = f\left(b_m + \sum_{k=0}^{n} w_{mk} x_k\right). \quad (14)$$

The training architecture, or training algorithm, is responsible for updating the weights of the network. There are different training architectures. The regularization techniques, like Levenberg-Marquardt (LM) and Bayesian regularization (BR), allow obtaining lower errors than other algorithms applied in approximation problems [49]. Bui et al. [50] describe LM and BR techniques.

The way data are entered into networks affects their training. An extensive database increases the number of patterns required for training and, therefore, the network's complexity. There are several recommendations to achieve a better trained ANN [51, 52], For example, reducing the sample size using statistical analysis and combining the number of variables to optimize the number of input and output variables [53], starting with a greater number of input variables and fewer neurons [54], or the scaling of data in a specific interval. Rafiq [55] proposed scaling in the interval [0, 1] or [−1, +1] by methods like linear normalization, as shown in equation (15). The data normalization into the range [−1, 1] would raise network training convergence because this range is the most sensitive for the variables' sigmoid functions [55, 56].

$$S = \frac{X - X_{\min}}{X_{\max} - X_{\min}}, \quad (15)$$

where S is the normalized value of the variable X, and $X_{\min}$ and $X_{\max}$ are the minimum and maximum values of the variable, respectively.

Once the ANN are trained, it is necessary to validate the results. The most usual way to do this is by measuring the error, such as the mean absolute error, the root-mean-square error, or the mean square error (MSE) [55].

$$MSE = \frac{1}{n} \sum_{i=1}^{n} (y_i - \text{out}_i)^2, \quad (16)$$

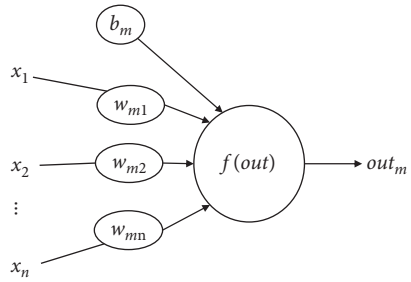

Figure 1: Perceptron scheme.

where n is the number of components of the output vector, y_i is the vector of desired output values, and out_i is the vector of output values predicted by the ANN.

In the present study, multilayer perceptron-based ANN are used, with unidirectional supervised learning, using a Sigmoid activation and transfer function and a linear output function. For the training, a database with unmodified (real) values and another database with normalized values are used in the training architectures Levenberg-Marquardt (LM) and Bayesian regularization (BR) using the Matlab tool [57]. The ANN are applied to obtain both demand and structural capacity factors and the structural reliability index implicit in steel wind turbine towers.

5. Case Study

Response surfaces were generated to obtain the structural reliability index, as well as the structural demand and structural capacity factors of wind turbine towers from the analysis results of 54 different steel towers' models. Likewise, ANN were trained to predict the same parameters.

The steel support towers were considered conical of variable diameter and thickness, based on S355 structural steel, with a modified density equal to 8500 kg/m3, which considers the contribution of accessories and screws. The rotor characteristics were considered the same for all tower models with a total weight of 836 kN and a diameter of 82.26 m.

It is considered the structure is located in an open terrain. Therefore, to simulate the wind forces on the tower, the auto-regressive moving average (ARMA) method [58] was applied at each meter of the tower's height. Concerning the force on the rotor, the blade element momentum (BEM) method was applied for the rotor in operation, while the simplified BEM method was applied for the standstill condition [59].

Figure 2 shows the steps followed, and later sections (5.1 to 5.4) detail each step.

5.1. Parametric Analysis of Stability and Buckling. As a first step, a parametric analysis of stability and buckling is performed to determine the support towers' acceptable geometry; it is carried out based on what is established by DNV-Riso [60] and Nicholson [61]. Different support tower geometries were tested [59] with heights of 70, 75, 80, and 85 m, lower and upper diameters of 3.0 to 4.5 m, and thicknesses of 2.5 to 4.5 cm.

The calculation of the displacement at the top of each tower model, the tower fundamental vibration frequency, the analysis of stability, and the tower's buckling at each meter was according to Section 7.4.7 of DNV-Risø [60]. For this purpose, the authors developed a program in Matlab [57].

The following conditions were verified to take as acceptable the configuration of the support tower:

(a) Maximum diameter allowed, 4.5 m

(b) Maximum thickness allowed, 0.040 m

(b) Diameter at top of the tower > width of the nacelle

(c) Tower natural frequency > rotor frequency

(d) Critical compressive stress > acting forces

(e) Displacement for a speed corresponding to a 50-year return period <3% of the tower's height, corresponding to the collapse limit state [62]

There were obtained 88,320 different models of steel support towers. From them, there were selected 54 models that covered heights from 70 to 85 m, fundamental periods between 1.5 s and 3.0 s, and values of acceptable diameters and thicknesses. Table 11 shows the geometric characteristics of the 54 models, the fundamental vibration period, and the lateral force associated with the collapse design velocity, equal to 50 m/s.

5.2. Reliability Analysis. For each model, a structural reliability analysis was performed, solving equations (2) to (10) to obtain the structural capacity factor, the structural demand factor, the structural reliability index, and the confidence factor. The structural capacity was determined from the capacity curves obtained from 15 nonlinear incremental dynamic analyses (IDAs). The process was repeated 10 times, resulting in 810 structural reliability analyses.

The median of the structural capacity, the structural demand, and their respective uncertainties were obtained using capacity curves represented by tower's top displacement versus mean wind speed. An expected annual probability of failure, ν_o equal to 0.0036, was selected [63]. The parameters r and b, obtained for the 54 models, were between 12 and 14 and between 6 and 8, respectively.

The results of the reliability analysis are represented with black dots in Figures 3–7. Also, they were used to form a database of 810 x11 elements, where each row corresponded to the results of the reliability analysis of a specific model, and the columns corresponded to the height, diameter, thickness, structural vibration period, lateral force, structural capacity factor, structural demand factor, reliability index, and confidence factor. The database was used to create the response surfaces, as well as to train the ANN.

5.3. Response Surface Method (RSM). The main objective of response surface is that from simple variables, such as height, structural period, or geometry, complex parameters such as reliability index and the demand and structural capacity factors can be estimated as a function of a preset probability

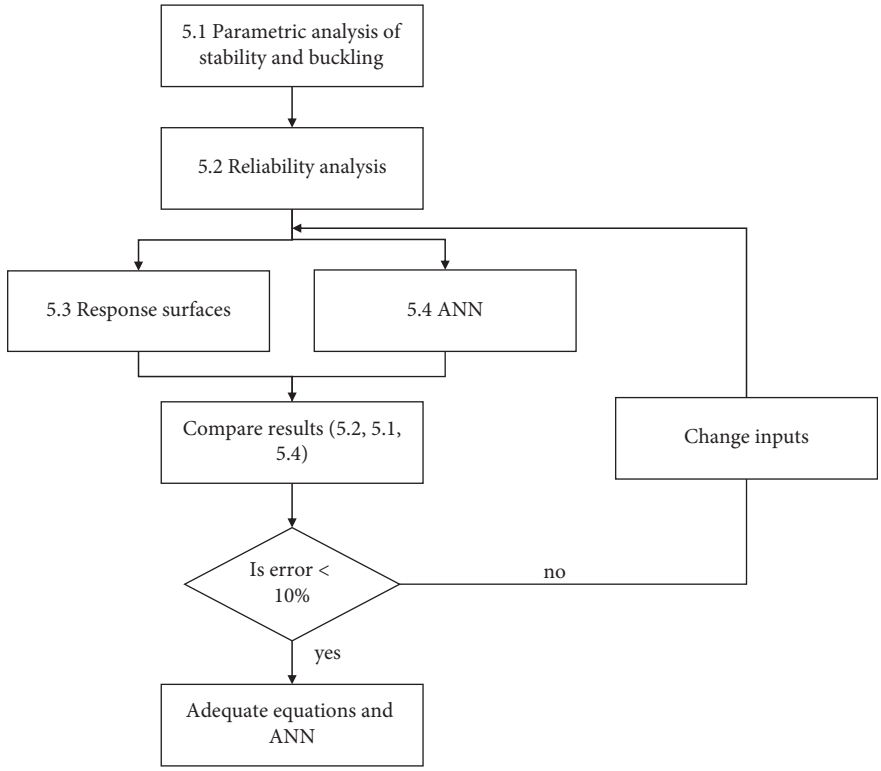

Figure 2: General methodology.

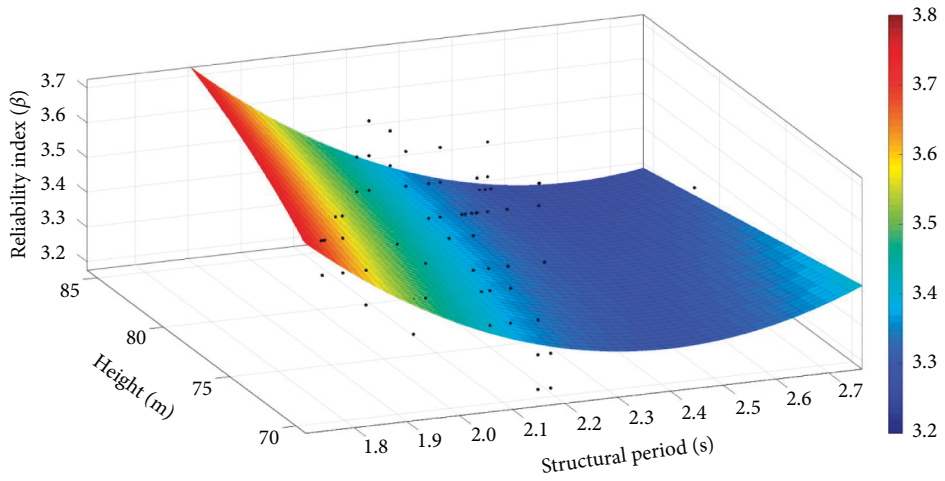

Figure 3: Reliability index vs structural vibration period and height.

of annual failure. Table 1 lists the variables in the database with their corresponding notation.

To obtain the response surface, two different variables were related in polynomials up to the second degree. The coefficients of the equations were obtained using the least-squares method. Finally, the combination of variables that showed the highest coefficient of determination $R2$ was chosen, which indicates the model's quality to replicate the results and their variations.

Tables 2–4 show the correlation coefficients obtained from three response surfaces for the structural capacity factor, the structural demand factor, and the structural reliability index, respectively. Remarkably, the combination of the fundamental structural vibration period and the tower height yields a higher coefficient of determination with a second-degree equation to obtain the factors of capacity and of structural demand; on the other hand, to obtain the reliability index, the variables that yield a higher coefficient of determination are the fundamental structural vibration period and the lateral force. For higher-degree equations, the coefficient of determination tends to be higher; however, the equation becomes less comfortable for its application from an engineering point of view.

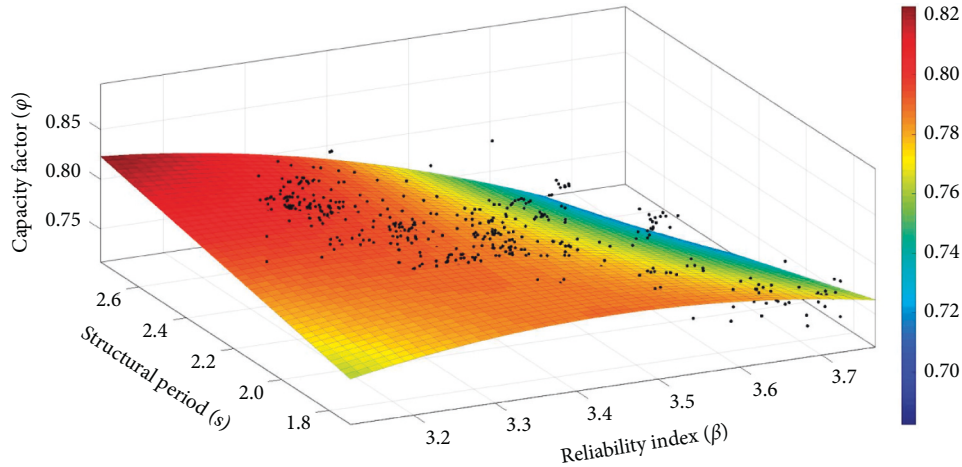

Figure 4: Capacity factor vs reliability index and structural vibration period.

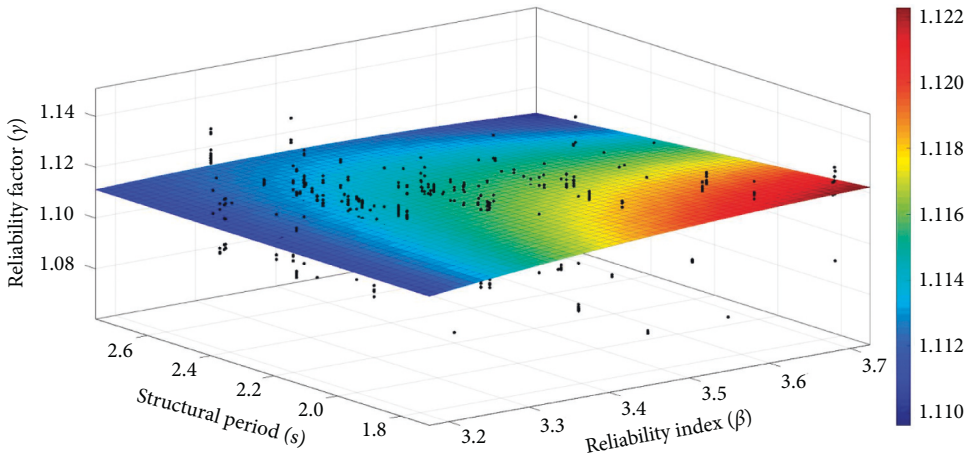

Figure 5: Demand factor vs reliability index and structural vibration period.

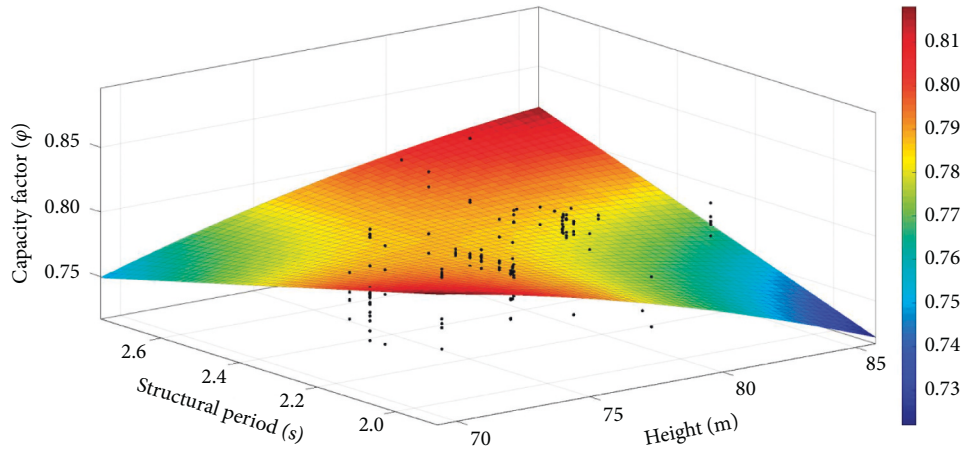

Figure 6: Capacity factor vs height and structural vibration period, corresponding to $\beta = 3.4$.

5.4. Artificial Neural Networks (ANN). Alternatively, ANN were trained to predict the structural demand and capacity factors, as well as the structural reliability index. Analogously to what was done for the response surface, the variables that allowed the ANN to be trained with a higher coefficient of determination and a lower mean square error were chosen.

The results from Levenberg-Marquardt (LM) and Bayesian regularization (B-R) training architectures were compared. Two databases were used: one with exact data

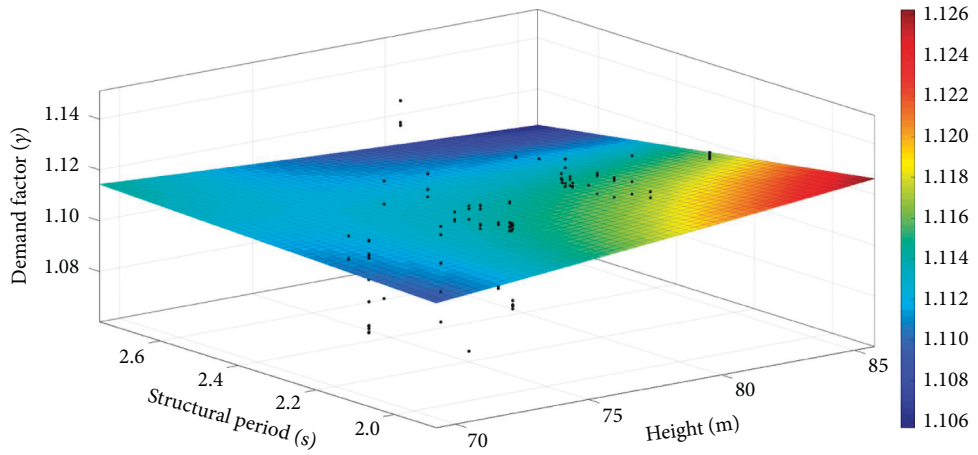

Figure 7: Demand factor vs height and structural vibration period, corresponding to $\beta = 3.4$.

Table 1: Input variables used for response surfaces and ANN.

Variable	
Height	x_1
Diameter at the base	x_2
Diameter at the top	x_3
Thickness at the base	x_4
Thickness at the top	x_5
Structural vibration period	x_6
Lateral force	x_7
Capacity factor	x_8
Demand factor	x_9
Reliability index	x_{10}
Confidence factor	x_{11}

Table 2: Coefficient of determination for the structural capacity factor.

		$\varphi = \mathbf{A} + \mathbf{Bx} + \mathbf{Cy}$	$\varphi = \mathbf{A} + \mathbf{Bx} + \mathbf{Cy} + \mathbf{Dx}^2 + \mathbf{Exy}$	$\varphi = \mathbf{A} + \mathbf{Bx} + \mathbf{Cy} + \mathbf{Dx}^2 + \mathbf{Exy} + \mathbf{Fy}^2$
$x = x_1$	$y = x_2$	0.2180	0.2705	0.2887
	$y = x_3$	0.2889	0.3193	0.3629
	$y = x_4$	0.1317	0.2438	0.2462
	$y = x_5$	0.1156	0.2052	0.1984
	$y = x_6$	0.3253	0.3186	0.4224
	$y = x_7$	0.1673	0.2094	0.2072
	$y = x_{10}$	0.3051	0.3539	0.3671
$x = x_6$	$y = x_1$	0.3110	0.4232	0.4224
	$y = x_7$	0.3293	0.3111	0.3109
	$y = x_{10}$	0.3485	0.3813	0.3790
$x = x_{10}$	$y = x_1$	0.3051	0.3388	0.3671
	$y = x_6$	0.3485	0.3839	0.3790

Table 3: Coefficient of determination for the structural demand factor.

		$\gamma = \mathbf{A} + \mathbf{Bx} + \mathbf{Cy}$	$\gamma = \mathbf{A} + \mathbf{Bx} + \mathbf{Cy} + \mathbf{Dx}^2 + \mathbf{Exy}$	$\gamma = \mathbf{A} + \mathbf{Bx} + \mathbf{Cy} + \mathbf{Dx}^2 + \mathbf{Exy} + \mathbf{Fy}^2$
$x = x_1$	$y = x_2$	0.5874	0.5766	0.5595
	$y = x_3$	0.4943	0.5247	0.5839
	$y = x_4$	0.4616	0.5384	0.5519
	$y = x_5$	0.4518	0.4451	0.4442
	$y = x_6$	0.5736	0.5672	0.6515
	$y = x_7$	0.4600	0.4560	0.4501
	$y = x_{10}$	0.5282	0.5786	0.5755
$x = x_6$	$y = x_1$	0.5736	0.6608	0.6515
	$y = x_7$	0.5326	0.5244	0.5186
	$y = x_{10}$	0.5439	0.5509	0.5442
$x = x_{10}$	$y = x_1$	0.5282	0.5244	0.5755
	$y = x_6$	0.5439	0.5321	0.5442

Table 4: Coefficient of determination for the structural reliability index.

		$\beta = \mathbf{A} + \mathbf{Bx} + \mathbf{Cy}$	$\beta = \mathbf{A} + \mathbf{Bx} + \mathbf{Cy} + \mathbf{Dx}^2 + \mathbf{Exy}$	$\beta = \mathbf{A} + \mathbf{Bx} + \mathbf{Cy} + \mathbf{Dx}^2 + \mathbf{Exy} + \mathbf{Fy}^2$
$x = x_1$	$y = x_2$	0.4378	0.4654	0.465
	$y = x_3$	0.6334	0.7005	0.7221
	$y = x_4$	0.3257	0.3912	0.4457
	$y = x_5$	0.2706	0.3394	0.3550
	$y = x_6$	0.6953	0.7060	0.7462
	$y = x_7$	0.4567	0.4979	0.4968
$x = x_6$	$y = x_1$	0.6953	0.7457	0.7462
	$y = x_7$	0.7241	0.7840	0.7840

obtained from the reliability analysis and the other with normalized data using (15). Finally, it was concluded that the databases with exact numbers and the Levenberg-Marquardt training architecture resulted in values closer to the median value of the structural capacity and demand factors and also closer to the verification models' reliability index. Tables 5 and 6 show the coefficient of determination and the mean square error of the trained ANN.

6. Comparison of Methods

6.1. Response Surface Method. The main objective of the response surfaces proposed in this section is to evaluate the reliability index, as well as the demand and capacity factors, of an installed structure, by means of simple parameters such as the structural vibration period (x) and its height (y). The reliability index obtained from the 54 models is represented in equation (17) and in Figure 3.

$$\begin{aligned} \beta &= 4.219 - 0.5557x + 5.209 \times 10^{-3} y, \quad \text{for } y = 70 \text{ and } 75\, m, \\ \beta &= 5.11 - 0.01336x - 0.2804y, \quad \text{for } y = 80 \text{ and } 85\, m. \end{aligned} \tag{17}$$

Once the reliability index was obtained, the structural capacity factor and the structural demand factor could be determined as a function of the reliability index (x) and the structural vibration period (y), as shown in (18) and (19) and in Figures 4 and 5. The main objective of these response surfaces is to obtain the capacity and demand factor required to achieve the desired reliability index, given the fundamental structural vibration period of the steel support tower.

$$\varphi = -3.25 + 1.995x + 0.7105y - 0.2374x^2 - 0.2093xy, \tag{18}$$

$$\gamma = 0.4536 + 0.3268x + 0.07116y - 0.03836x^2 - 0.02169xy. \tag{19}$$

Besides, response surfaces were obtained to determine the capacity factor and the structural demand factor necessary to achieve a desirable structural reliability index equal to $\beta = 3.4$ [63], as a function of the tower's height (x) and the structural vibration period (y). This is shown in equations (20) and (21) and in Figures 6 and 7.

$$\begin{aligned} \varphi = {} & 2.106 - 7.196 \times 10^{-3} x - 0.8849y \\ & - 1.33 \times 10^{-4} x^2 + 0.01162xy, \end{aligned} \tag{20}$$

$$\begin{aligned} \gamma = {} & 0.8213 + 3.642 \times 10^{-3} x + 0.1306y + 5.126 \\ & \times 10^{-6} x^2 - 1.801 \times 10^{-3} xy. \end{aligned} \tag{21}$$

6.2. Artificial Neural Networks. Similar to the response surfaces, the main objective of the ANN is to obtain the reliability index of the existing structure, starting from simple parameters and avoiding excessive computing hours or complicated structural analyses.

The ANN were trained here using the database of the 54 models selected and using ten hidden layers and random samples for training, validation, and testing with a ratio of 70%, 15%, and 15% of the total database, respectively. After the testing, the results were verified with three different models whose characteristics are shown in Table 7 and were not found among the 54 models.

To predict the structural reliability index β, the following input parameters were used: tower's height, structural fundamental vibration period, lateral force associated with a 50-year return period, and the desirable confidence factor should be greater than 1.0. Figure 8 shows results of the reliability index calculated from 10 reliability analyses (Equations (2) to (10)) for the three verification models, as well as the ANN training results.

The following input parameters were used to predict the structural capacity factor: tower's height, structural vibration period, lateral force associated with a 50-year return period, structural reliability index, confidence factor, and displacement at the top of the tower, corresponding to the collapse limit state. Figure 9 shows the three verification models' reliability analysis results for the capacity factor and those predicted with ANN.

The following input parameters were used to predict the structural demand factor: the tower's height, the structural vibration period, and the structural capacity factor. Figure 10 shows the three verification models' reliability analysis results and those predicted with ANN.

Table 8 compares the median value of the structural capacity factor, the structural demand factor, and the reliability index obtained from 10 reliability analyses (Equations (2) to (10)) for the three verification models, with the value obtained from the proposed equations and with ANN,

Table 5: ANN coefficient of determination, $R2$.

	LM		B-R	
ANN	Real database	Normalized database	Real database	Normalized database
Capacity factor	0.9436	0.4767	0.9179	0.2550
Demand factor	0.9771	0.1580	0.9953	0.9773
Reliability index	0.9874	0.9321	0.01	0.20

Table 6: Mean square error of ANN.

	LM		B-R	
ANN	Real database	Normalized database	Real database	Normalized database
Capacity factor	0.007	0.012	0.030	0.020
Demand factor	0.001	0.0054	0.002	0.002
Reliability index	0.011	0.027	0.18	0.17

Table 7: Characteristics of the verification models.

Height (m)	# of model	Diameter at base (m)	Diameter at top (m)	Thickness at base (cm)	Thickness at top (cm)	Structural period (s)	Lateral force (MN)
70	14	4.00	2.20	3.65	3.10	2.11	1.504
75	16	4.00	2.50	3.81	2.60	2.27	1.492
80	16	4.30	2.55	3.81	2.50	2.31	1.593

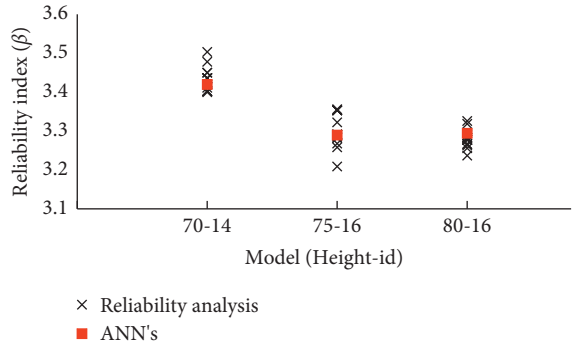

Figure 8: Structural reliability index corresponding to the verification models.

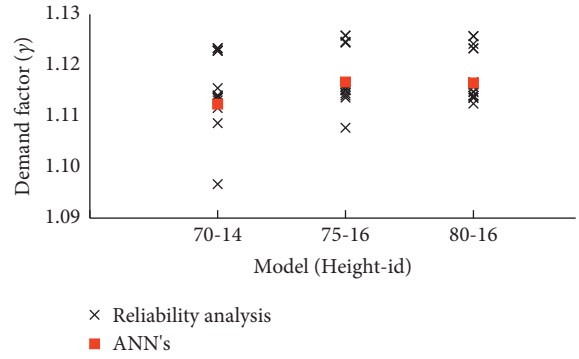

Figure 10: Structural demand factors corresponding to the verification models.

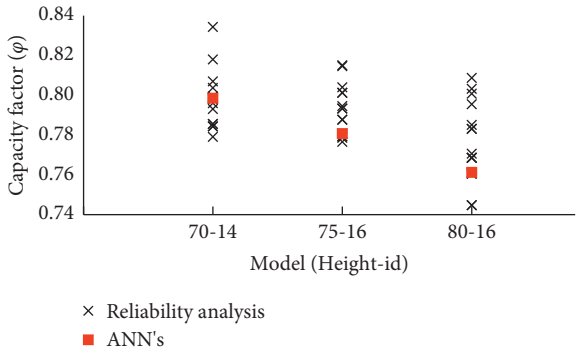

Figure 9: Structural capacity factors corresponding to the verification models.

respectively. The first column 1 in Table 8 corresponds to the tower's height, column 2 is an identifying model number, column 3 indicates the fundamental structural vibration period, and columns 4, 5, 6, and 7 show results obtained from the reliability analyses (column 4), from the equations proposed in this study (columns 5–6), and from ANN predictions (column 7). The coefficient of determination (R2) and the mean square error (MSE) of the equations and ANN are also shown, compared to the reliability analyses results. Tables 9 and 10 show similar results for the structural demand factor and the structural reliability index.

Table 8 shows that, for the three verification models, ANN give place to greater accuracy for the capacity factor ($R2 = 0.96$), with an MSE six times smaller than that corresponding to equation (18) and 30% smaller than that to equation (20). Similarly, the reliability index obtained with ANN presents a higher R2 value than that corresponding to equation (17) (0.93 vs. 0.45), and an MSE value is eight times smaller (see Table 10). Even though for the structural demand factor obtained with ANN, the value of R2 is slightly smaller (1%) than that obtained with equation (19), and an

Table 8: Comparison of structural capacity factor results.

MODEL		Structural capacity factor				
(1) Height (m)	(2) Model ID	(3) Structural period (s)	(4) Reliability analysis	(5) Equation (18)	(6) Equation (20) $\beta = 3.4$	(7) ANN
70	14	2.106	0.798	0.784	0.800	0.798
75	16	2.267	0.790	0.794	0.788	0.781
80	16	2.308	0.769	0.795	0.782	0.761
			R2	0.64	0.80	0.96
			ECM	1.06X10-4	9.27X10-5	7.25X10-5

Table 9: Comparison of structural demand factor results.

MODEL		Structural	Structural demand factor			
Height (m)	ID	period (s)	Reliability analysis	Equation (19)	Equation (21) $\beta = 3.4$	ANN
70	14	2.106	1.114	1.116	1.111	1.112
75	16	2.267	1.116	1.113	1.113	1.117
80	16	2.308	1.116	1.113	1.114	1.117
			R2	0.99	0.94	0.98
			ECM	1.16X10-5	9.10X10-6	1.78X10-6

Table 10: Comparison of reliability index results.

MODEL		Structural period (s)	Structural reliability index		
Height (m)	ID		Reliability analysis	Equation (17)	ANN
70	14	2.106	3.43	3.413	3.41
75	16	2.267	3.29	3.350	3.25
80	16	2.308	3.28	3.394	3.28
			$R2$	0.45	0.93
			ECM	$8.70X10-3$	$1.08X10-3$

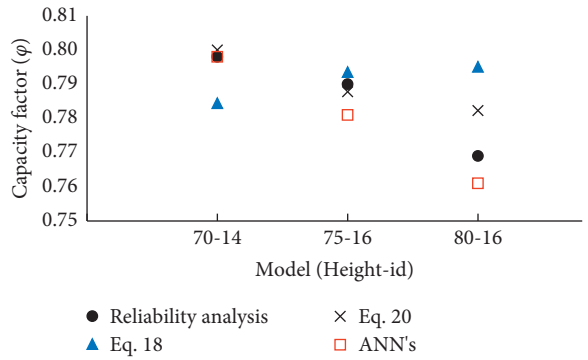

Figure 11: Comparison of results for the capacity factor.

MSE value is five times smaller. Therefore, for the cases studied here, it is concluded that ANN results lead to greater accuracy than those obtained with the RSM (see Table 9).

Figures 11–13 show the results of Tables 8–10, respectively; it is clear that the results predicted by the ANN are more accurate than the results obtained by the response surfaces. This is because the training of ANN involves a greater number of variables for predicting the reliability parameters.

In Figure 11, it can be observed that for the 70–14 model, the ANN result does not present any difference for the capacity factor value obtained from the reliability analysis, while those calculated with (18) and with (20) present relative errors of 1.7% and 0.25%, respectively. For the 75–16 model, (20) leads to a smaller relative error (0.28%) than that corresponding to equation (18) (0.45%) and to ANN (1.14%). For the 80–16 model, the ANN present a smaller error (1.04%) than those corresponding to equations (18) and (20) (3.39% and 1.73%, respectively). In conclusion, for the cases corresponding to the structural capacity factor evaluation, ANN allow obtaining values with smaller errors than RSM.

In Figure 12, it can be seen that for 70–14 model, the ANN present a difference of 0.13% with respect to the structural demand factor value obtained from the reliability

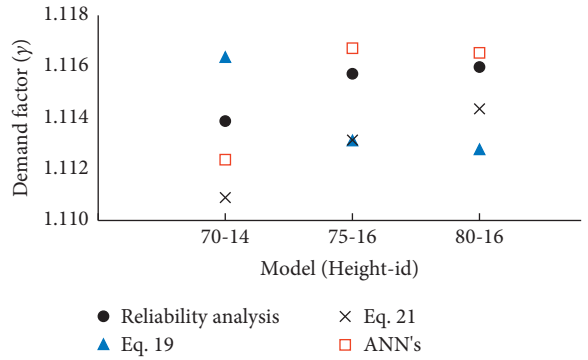

Figure 12: Comparison of results for the demand factor.

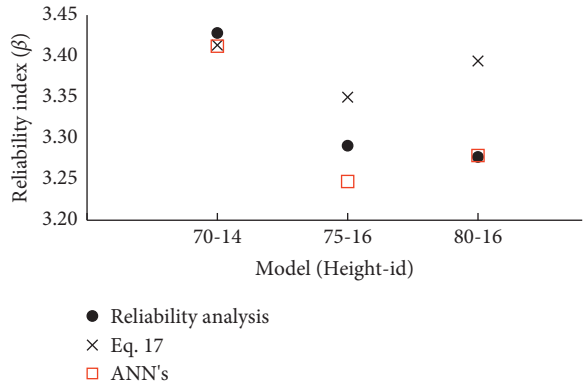

Figure 13: Comparison of results for the structural reliability index.

Table 11: Characteristics of the models used in the database.

Height (m)	# of model	Diameter at the base (m)	Diameter at the top (m)	Thickness at the base (cm)	Thickness at the top (cm)	Structural fundamental period (s)	Lateral force (MN)
70	1	4.5	2.35	3.18	2.1	1.93	1.627
70	2	4.5	2.75	3.65	2.5	1.76	1.595
70	3	4.4	2.9	3.33	2.2	1.84	1.631
70	4	4.4	3.3	3.49	2.8	1.76	1.663
70	5	4.1	2.55	3.81	3.1	1.95	1.582
70	6	4.1	2.05	3.49	3	2.11	1.542
70	7	3.9	1.95	3.97	3.2	2.17	1.520
70	8	3.9	2.35	3.81	2.7	2.11	1.551
70	9	3.8	2.7	3.97	2.8	2.08	1.571
70	10	3.8	2.1	3.97	3.4	2.19	1.524
70	11	3.8	2.8	3.97	3.4	2.06	1.471
70	12	4.5	3.35	3.18	2.9	1.76	1.546
70	13	4.5	3.35	3.02	1.9	1.80	1.546
75	1	4.5	2.25	3.49	2.7	2.09	1.638
75	2	4.5	3.25	3.49	2.3	1.92	1.727
75	3	4.3	2.65	3.65	2.5	2.09	1.658
75	4	4.3	3.05	3.65	3.3	2.03	1.693
75	5	4.2	2.1	3.97	2.8	2.20	1.601
75	6	4.2	2.75	3.65	3.1	2.12	1.658
75	7	4.1	2.65	3.81	3	2.17	1.641
75	8	4.1	2.35	3.8	2.6	2.24	1.615
75	9	3.9	2.75	3.97	2.8	2.25	1.634
75	10	3.9	2.45	3.97	3.2	2.30	1.573
75	11	3.9	2.85	3.97	3.6	2.24	1.509
75	12	4.1	2.05	3.97	3.6	2.25	1.470
75	13	4.5	2.45	3.33	2.1	2.09	1.495
75	14	4.5	3.35	3.49	2.3	1.91	1.577

Table 11: Continued.

Height (m)	# of model	Diameter at the base (m)	Diameter at the top (m)	Thickness at the base (cm)	Thickness at the top (cm)	Structural fundamental period (s)	Lateral force (MN)
75	15	4.5	2.45	3.33	2.1	2.09	1.519
80	1	4.5	2.45	3.8	2.5	2.71	1.733
80	2	4.5	3.35	3.65	2.8	2.10	1.815
80	3	4.4	2.2	4	2.9	2.28	1.702
80	4	4.4	2.8	3.65	2.6	2.23	1.756
80	5	4.3	3.15	3.8	3.1	2.21	1.780
80	6	4.3	2.75	3.65	2.6	2.30	1.744
80	7	4.2	2.4	4	2.9	2.36	1.703
80	8	4.2	2.9	3.81	2.7	2.30	1.749
80	9	4.1	3.05	3.97	3.5	2.32	1.754
80	10	4.1	2.45	3.97	3.3	2.42	1.699
80	11	4.5	2.45	3.5	2.6	2.27	1.733
80	12	4.50	2.45	4	3.5	2.17	1.733
80	13	4.5	2.25	3.65	2.4	2.29	1.586
80	14	4.5	3.35	3.49	2.2	2.12	1.661
80	15	4.5	3.35	3.81	3.1	2.07	1.661
85	1	4.5	2.25	3.97	3.2	2.44	1.668
85	2	4.5	2.85	3.49	2.2	2.43	1.726
85	3	4.5	3.35	3.97	3	2.26	1.774
85	4	4.4	2.4	3.65	3	2.55	1.673
85	5	4.4	3	3.81	2.5	2.39	1.731
85	6	4.4	3.3	3.65	2.4	2.38	1.760
85	7	4.3	2.55	3.81	3.3	2.55	1.679
85	8	4.3	2.85	3.97	2.8	2.45	1.708
85	9	4.3	3.15	3.97	3.4	2.42	1.737
85	10	4.5	2.75	3.65	2.3	2.42	1.573
85	11	4.5	2.55	3.81	2.7	2.42	1.559

analysis, while (19) and (21) give place to relative errors of 0.22% and 0.27%, respectively. For the 75–16 model, the ANN present a smaller relative error (0.09%) than that obtained from equations (19) and (21) (both 0.23%). For the 80–16 model, ANN present an error (0.05%) which is smaller than that obtained from equations (19) and (21) (0.29% and 0.15%, respectively). Thus, in general, for the structural demand factor evaluation, ANN give place to values with minor errors than those corresponding to RSM.

Figure 13 shows that for 70–14 model, the ANN present a difference with respect to the structural reliability index value obtained from the reliability analysis equal to 0.47%, while (17) gives place to a relative error of 0.43%. For the 75–16 and 80–16 models, the ANN present smaller relative errors (1.32% and 0.05%, respectively) than those corresponding to equation (17) (1.80% and 3.57%, respectively). It is concluded that for the structural reliability index evaluation, ANN allow obtaining values with minor errors than those obtained with RSM.

7. Conclusions

Response surface and ANN methods allow estimating the structural reliability index as well as the structural demand and capacity factors of wind turbine towers, using basic variables. The results obtained from the present study are valid for support towers with similar characteristics to those described in Table 11 and installed inland in open terrain; however, the proposed methodology may apply to another type of structures.

With the ANN trained in this study, it is possible to evaluate the structural reliability index and the demand and structural capacity factors inherent in steel wind turbine towers like those located in La Ventosa, Mexico.

The response surfaces proposed in this study allow obtaining the reliability index inherent to the structure as a function of its height and fundamental structural vibration period, as well as obtaining the demand and structural capacity factors required to reach the desired reliability level, given the fundamental structural vibration period and the tower's height.

For the wind turbine towers analyzed here, the ANN, trained with the Levenberg-Marquardt algorithm and a database with the exact values obtained from the reliability analysis, it was possible to predict more accurately the structural reliability index, as well as the demand and structural capacity factors, than when the Response Surface method was used. This result is because ANN recognize patterns of behavior and involve a larger number of variables in solving a problem.

To achieve a good training of ANN, it is necessary to have a wide database in which extreme and intermediate data of the variables involved are considered, as well as the choice of the appropriate number of input variables for the training of the network, since a large number of variables will tend to over-training or slow down the learning process. Likewise, uniformity must be maintained in the magnitude of the data, that is, although the input data units are different, they must have the same order of magnitude.

This study is a part of an ongoing research. Future works intend to expand the number of variables such as rotor area, type of terrain, and wind potential, as well as to consider different heights of support towers. In addition, ANN will be used in future research studies to predict the structural performance as well as to optimize the structural design of wind turbine towers, taking into account variables such as structural reliability index, the total cost of the structure, and wind potential.

Appendix

Table 11 shows the geometric characteristics of the 54 models that conform to the database, such as the tower's height (column 1), an identification number for the model (column 2), diameter at the base and the top of the tower (column 3 and 4, respectively), thickness at the base and the top of the tower (column 5 and 6, respectively), and other characteristics as the fundamental vibration period (column 7) and the lateral force associated with the collapse design velocity, equal to 50 m/s (column 8).

Data Availability

The data supporting the results can be obtained under request to the first author.

Conflicts of Interest

The authors declare that they have no conflicts of interest.

Acknowledgments

This research was done with the support of DGAPA-UNAM under project PAPIIT-IN100320. Thanks are due to PASPA-DGAPA-UNAM for the support given to the second author during her academic stay at the Instituto Tecnológico de Ciudad Madero.

References

[1] C. A. Cornell, F. Jalayer, R. O. Hamburger, and D. A. Foutch, "Probabilistic basis for 2000 SAC federal emergency management agency steel moment frame guidelines," *Journal of Structural Engineering*, vol. 128, no. 4, pp. 526–533, 2002.

[2] B. R. Ellingwood and P. B. Tekie, "Wind load statistics for probability-based structural design," *Journal of Structural Engineering*, vol. 125, no. 4, pp. 453–463, 1999.

[3] K. O. Ronold and C. J. Christensen, "Optimization of a design code for wind-turbine rotor blades in fatigue," *Engineering Structures*, vol. 23, no. 8, pp. 993–1004, 2001.

[4] L. D'Angelo and A. Nussbaumer, "New framework for calibration of partial safety factors for fatigue design," *Journal of Constructional Steel Research*, vol. 139, pp. 466–472, 2017.

[5] Y. G. Matvienko, "The simplified approach for estimating probabilistic safety factors in fracture mechanics," *Engineering Failure Analysis*, vol. 117, Article ID 104814, 2020.

[6] C. G. Bucher and U. Bourgund, "A fast and efficient response surface approach for structural reliability problems," *Structural Safety*, vol. 7, no. 1, pp. 57–66, 1990.

[7] H. P. Gavin and S. C. Yau, "High-order limit state functions in the response surface method for structural reliability analysis," *Structural Safety*, vol. 30, no. 2, pp. 162–179, 2008.

[8] A. Hadidi, B. F. Azar, and A. Rafiee, "Efficient response surface method for high-dimensional structural reliability analysis," *Structural Safety*, vol. 68, pp. 15–27, 2017.

[9] I. Kaymaz and C. A. McMahon, "A response surface method based on weighted regression for structural reliability analysis," *Probabilistic Engineering Mechanics*, vol. 20, no. 1, pp. 11–17, 2005.

[10] Z. Zhang, C. Jiang, X. Han, D. Hu, and S. Yu, "A response surface approach for structural reliability analysis using evidence theory," *Advances in Engineering Software*, vol. 69, pp. 37–45, 2014.

[11] R. Falcone, C. Lima, and E. Martinelli, "Soft computing techniques in structural and earthquake engineering: a literature review," *Engineering Structures*, vol. 207, Article ID 110269, 2020.

[12] V. Chandwani, V. Agrawal, and R. Nagar, "Applications of soft computing in civil engineering: a review," *International Journal of Computer Application*, vol. 81, no. 10, pp. 13–20, 2013.

[13] M. Papadrakakis, N. D. Lagaros, and V. Plevris, "Design optimization of steel structures considering uncertainties," *Engineering Structures*, vol. 27, no. 9, pp. 1408–1418, 2005.

[14] V. Plevris and M. Papadrakakis, "A hybrid particle swarm-gradient algorithm for global structural optimization," *Computer-Aided Civil and Infrastructure Engineering*, vol. 26, no. 1, pp. 48–68, 2010.

[15] N. D. Lagaros and M. Papadrakakis, "Neural network based prediction schemes of the non-linear seismic response of 3D buildings," *Advances in Engineering Software*, vol. 44, no. 1, pp. 92–115, 2012.

[16] K. Hornik, M. Stinchcombe, and H. White, "Multilayer feedforward networks are universal approximators," *Neural Networks*, vol. 2, no. 5, pp. 359–366, 1989.

[17] A. A. Chojaczyk, A. P. Teixeira, L. C. Neves, J. B. Cardoso, and C. Guedes Soares, "Review and application of Artificial Neural Networks models in reliability analysis of steel structures," *Structural Safety*, vol. 52, pp. 78–89, 2015.

[18] W. J. De Santana Gomes, "Structural reliability analysis using adaptive artificial neural networks," *ASCE-ASME Journal of Risk and Uncertainty in Engineering Systems, Part B: Mechanical Engineering*, vol. 5, no. 4, 2019.

[19] J. Cheng, "Hybrid genetic algorithms for structural reliability analysis," *Computers & Structures*, vol. 85, no. 19-20, pp. 1524–1533, 2007.

[20] J. Cheng and Q. S. Li, "Reliability analysis of structures using artificial neural network based genetic algorithms," *Computer Methods in Applied Mechanics and Engineering*, vol. 197, no. 45-48, pp. 3742–3750, 2008.

[21] J. Cheng, "An artificial neural network based genetic algorithm for estimating the reliability of long span suspension bridges," *Finite Elements in Analysis and Design*, vol. 46, no. 8, pp. 658–667, 2010.

[22] J. Bojórquez, S. E. Ruiz, B. Ellingwood, A. Reyes-Salazar, and E. Bojórquez, "Reliability-based optimal load factors for seismic design of buildings," *Engineering Structures*, vol. 151, pp. 527–539, 2017.

[23] H. Dai and Z. Cao, "A wavelet support vector machine-based neural network metamodel for structural reliability assessment," *Computer-Aided Civil and Infrastructure Engineering*, vol. 32, no. 4, pp. 344–357, 2017.

[24] K. Wen, L. He, J. Liu, and J. Gong, "An optimization of artificial neural network modeling methodology for the reliability assessment of corroding natural gas pipelines," *Journal of Loss Prevention in the Process Industries*, vol. 60, pp. 1–8, 2019.

[25] M. Koopialipoor, B. R. Murlidhar, A. Hedayat, D. J. Armaghani, B. Gordan, and E. T. Mohamad, "The use of new intelligent techniques in designing retaining walls," *Engineering with Computers*, vol. 36, no. 1, pp. 283–294, 2020.

[26] A. Zeroual, A. Fourar, and M. Djeddou, "Predictive modeling of static and seismic stability of small homogeneous earth dams using artificial neural network," *Arabian Journal of Geosciences*, vol. 12, no. 2, 2019.

[27] B. Gordan, M. Koopialipoor, A. Clementking, H. Tootoonchi, and E. Tonnizam Mohamad, "Estimating and optimizing safety factors of retaining wall through neural network and bee colony techniques," *Engineering with Computers*, vol. 35, no. 3, pp. 945–954, 2019.

[28] J. Zhang, J. Hu, X. Li, and J. Li, "Bayesian network based machine learning for design of pile foundations," *Automation in Construction*, vol. 118, Article ID 103295, 2020.

[29] L. Esteva, "Criterios para la construcción de espectros para diseño sísmico," in *Insituto de Materiales y Modelos Estructurales*, pp. 48–78, Facultad de Ingenieria, Universidad Central de Venezuela, Caracas, Venezuela, 1967.

[30] C. A. Cornell, "Engineering seismic risk analysis," *Bulletin of the Seismological Society of America*, vol. 58, no. 5, pp. 1583–1606, 1968.

[31] M. A. Torres and S. E. Ruiz, "Structural reliability evaluation considering capacity degradation over time," *Engineering Structures*, vol. 29, no. 9, pp. 2183–2192, 2007.

[32] D. Tolentino and S. E. Ruiz, "Time-dependent confidence factor for structures with cumulative damage," *Earthquake Spectra*, vol. 31, no. 1, pp. 441–461, 2015.

[33] H. M. Gomes and A. M. Awruch, "Comparison of response surface and neural network with other methods for structural reliability analysis," *Structural Safety*, vol. 26, no. 1, pp. 49–67, 2004.

[34] T. Hill, L. Marquez, M. O'Connor, and W. Remus, "Artificial neural network models for forecasting and decision making," *International Journal of Forecasting*, vol. 10, no. 1, pp. 5–15, 1994.

[35] O. I. Abiodun, A. Jantan, A. E. Omolara, K. V. Dada, N. A. Mohamed, and H. Arshad, "State-of-the-art in artificial neural network applications: a survey," *Heliyon*, vol. 4, no. 11, Article ID e00938, 2018.

[36] W. S. McCulloch and W. Pitts, "A logical calculus of the ideas immanent in nervous activity," *Bulletin of Mathematical Biophysics*, vol. 5, no. 4, pp. 115–133, 1943.

[37] P. M. Buscema, G. Massini, M. Breda, W. A. Lodwick, and F. Newman, *Artificial Adaptive Systems Using Auto Contractive Maps*, Springer, Berlin, Germany, 2018.

[38] X. Wang, X. Lin, and X. Dang, "Supervised learning in spiking neural networks: a review of algorithms and evaluations," *Neural Networks*, vol. 125, pp. 258–280, 2020.

[39] H. U. Dike, Y. Zhou, K. K. Deveerasetty, and Q. Wu, "Unsupervised learning based on artificial neural network: a review," in *Proceedings of the IEEE International Conference on Cyborg and Bionic Systems (CBS)*, pp. 322–327, Shenzhen, China, October 2018.

[40] L. R. Medsker and L. R. Medsker, "Hybrid neural network and expert systems," *Malaysian Journal of Computer Science*, vol. 12, 2012.

[41] A. Behnood and E. M. Golafshani, "Predicting the compressive strength of silica fume concrete using hybrid artificial neural network with multi-objective grey wolves," *Journal of Cleaner Production*, vol. 202, pp. 54–64, 2018.

[42] R. Lu, S. H. Hong, and M. Yu, "Demand response for home energy management using reinforcement learning and artificial neural network," *IEEE Transactions on Smart Grid*, vol. 10, no. 6, pp. 6629–6639, 2019.

[43] B. Baker, O. Gupta, N. Naik, and R. Raskar, "Designing neural network architectures using reinforcement learning," in *Proceedings of the 5th Int. Conf. Learn. Represent. ICLR 2017 - Conf. Track Proc*, pp. 1–18, Toulon, France, April 2017.

[44] F. Rosenblatt, "The perceptron: a probabilistic model for information storage and organization in the brain," *Psychological Review*, vol. 65, no. 6, pp. 386–408, 1958.

[45] M. M. Minsky and S. A. Papert, *Perceptons: An Introduction to Computational Geometry*, Cambrige Mass, MIT Press, Cambrige, MA, USA, 1988.

[46] M. Schuld, I. Sinayskiy, and F. Petruccione, "Simulating a perceptron on a quantum computer," *Physics Letters A*, vol. 379, no. 7, pp. 660–663, 2015.

[47] M. T. Camacho Olmedo, M. Paegelow, J. F. Mas, and F. Escobar, *Geomatic Approaches for Modeling Land Change Scenarios*Springer, Berlin, Germany, 2018.

[48] C. M. Bishop, *Neural Networks for Pattern Recognition*, Oxford University Press, UK, 1995.

[49] H. Demuth, "Neural network toolbox TM 6 user ' s guide," vol. 94 pages, 2000.

[50] D. Tien Bui, B. Pradhan, O. Lofman, I. Revhaug, and O. B. Dick, "Landslide susceptibility assessment in the Hoa Binh province of Vietnam: a comparison of the Levenberg-Marquardt and Bayesian regularized neural networks," *Geomorphology*, vol. 171-172, pp. 12–29, 2012.

[51] L. Lean Yu, S. Shouyang Wang, and K. K. Lai, "An integrated data preparation scheme for neural network data analysis," *IEEE Transactions on Knowledge and Data Engineering*, vol. 18, no. 2, pp. 217–230, 2006.

[52] S. I. Koval, "Data preparation for neural network data analysis," in *Proceedings of the IEEE Conference of Russian Young Researchers in Electrical and Electronic Engineering (EIConRus)*, vol. 2018, pp. 898–901, Moscow and St. Petersburg, Russia, January 2018.

[53] R. Stein, "Selecting data for neural networks," *AI Expert*, vol. 8, 1993.

[54] K. Swingler, *Applying Neural Networks a Practical Guide*, Academic Press, New York, NY, USA, 1996.

[55] M. Y. Rafiq, G. Bugmann, and D. J. Easterbrook, "Neural network design for engineering applications," *Computers & Structures*, vol. 79, no. 17, pp. 1541–1552, 2001.

[56] W. Zhao, M. Egusquiza, C. Valero, D. Valentín, A. Presas, and E. Egusquiza, "On the use of artificial neural networks for condition monitoring of pump-turbines with extended operation," *Measurement*, vol. 163, Article ID 107952, 2020.

[57] Matlab, *Matlab R2014b, , Student License*, Mathworks Inc., Massachusetts, MA, USA, 2014.

[58] E. Samaras, M. Shinzuka, and A. Tsurui, "ARMA representation of random processes," *Journal of Engineering Mechanics*, vol. 111, no. 3, pp. 449–461, 1985.

[59] I. Inzunza-Aragón and S. E. Ruiz, "Capacity and Demand Factors changing over time. Application to wind turbine steel towers," *Engineering Structures*, vol. 206, Article ID 110156, 2020.

[60] Dnv/Riso, *Guidelines for Design of Wind Turbines*, 2nd ed. edition, 2002.

[61] J. C. Nicholson, *Design of Wind Turbine tower and Foundation Systems: Optimization Approach*, University of Iowa, Iowa City, USA, 2011.
[62] A. R. Vaghela and G. S. Doiphode, "Door opening analysis of wind turbine steel tubular tower," *International Journal of Renewable Energy Technology*, vol. 3, no. 5, pp. 491–496, 2014.
[63] H. F. Veldkamp, *Chances in Wind Energy. A Probabilistic Approach to Wind Turbine Fatigue Design*, Delf Technical University, Delft, Netherlands, 2006.